J Inorg Organomet Polym (2017) 27:1450–1456
DOI 10.1007/s10904-017-0600-2

Green Synthesis and Characterization of Halloysite Nanoclay/Curcumin/Ag Hybrid Nano Materials for Antibacterial Applications

K. Sudhakar[1] · S. J. Moloi[1] · K. Madhusudhana Rao[2]

Received: 24 February 2017 / Accepted: 15 June 2017 / Published online: 22 June 2017

Abstract In this report a new method to produce silver nanoparticles (AgNPs) in the intercalation of highly biocompatible halloysite nanoclay (HNTs) has been produced using curcumin as a reducing agent. AgNPs are stable in the lumen structure and also in the silicate cage of HNTs. The intercalation of halloysite of curcumin and of AgNPs was confirmed by Fourier transform infrared spectroscopy and the formation of AgNPs was investigated by UV–Visible spectroscopy. The crystallinity of AgNPs in HNTs was investigated by X-ray diffraction technique. The morphology of AgNPs in HNTs was investigated by scanning electron microscopy and transmission electron microscopy techniques. Energy dispersive spectroscopy and X-ray photonelectron spectroscopy techniques were used to determine the quantification and compositional elements in HNTs/cur/AgNPs. Furthermore, the antimicrobial efficiency of AgNPs on Gram-positive *Bacillus cereus* and on Gram-negative *Escherichia coli* bacteria was studied using the diameter of inhibition zone in the disk diffusion test.

Keywords Halloysite · Curcumin · Silver nanoparticles · Antibacterial activity · *E.coli* · *Bacillus*

✉ K. Sudhakar
ksrsudhakar11@gmail.com; kunchs@unisa.ac.za

[1] Department of Physics, College of Science, Engineering &Technology, University of South Africa, Cnr Chrstiaan de Wet & Pioneer Streets, Private Bag X6, Johannesburg 1710, Florida, South Africa

[2] School of Chemical Engineering, Yeungnam University, 280-Daehak-Ro, Gyeongsan 712-749, South Korea

1 Introduction

The synthesis of sliver nanoparticles (AgNPs) has been drawn great attention of researchers due to their peculiar physical and chemical characteristics [1–3]. Intrinsic properties of AgNPs for various applications such as in optical, catalysis, and antimicrobial activity have been studied [4–6]. Due to its large surface area in nano form, its stable dispersion silver has been used to prevent spoilage and fight against microbial pathogens [7, 8]. There is however a need for development of nano hybrid material with an appropriate combination of AgNPs and other materials to fulfil challenges of characteristics in biomedical technology. Materials such as halloysite nanotubes (HNT) [9–11], activated carbon and carbon nanotubes [12–14], zeolites [15, 16], polymers [17, 18] and encapsulation by other materials [19–21] have been used for the preparation of AgNPs hybrid material. Among these, HNTs clay materials are much cheaper, most abundant, and highly biocompatible [22]. HNT clay materials exhibit exciting physical and chemical properties and retain the hollow tubular structure. In addition, HNTs have good dispersion property and can be easily modified due to their fewer hydroxyl groups on the surface area. The materials have been used as absorbent [23] and catalyst reinforcement [24]. It is with these reasons that HNTs are combined with AgNPs for production of nano hybrid material for medical applications.

Now days, chemical reductions, photo-catalytic reduction, gamma irradiation [25], electron irradiation microwave method [26], photo-chemical [27], polyols [28] and biological techniques [29] have been used for synthesis of AgNPs. Hybrid AgNPs are produced from modified clay materials by using conventional chemical method. Chemical reduction method, on the other hand, is toxic and harmful for living systems [30, 31]. For this reason, a green

reduced method has been chosen for production of AgNPs in this work. The AgNPs are produced from silver nitrate via insitu reduction using curcumin as a natural phenolic compound for reduction in this work. Curcumin is used due to its high pleotropic molecule that can interact with multi targets [32–34].

In this work, a simple two steps in green method were used for production of AgNPs with combination of HNTs and cur. First step being intercalation or complexation between HNTs and curcumin and another step is being insitu reduction for silver nitrate to form silver nano particles in HNTs. In the latter method curcumin was used as a strong reducing agent for silver nitrate. This is to form stable colloidal AgNPs in the lumen structure and in silicate cage of HNTs. The obtained HNTs/AgNPs hybrid materials were characterized by Fourier transform infrared spectroscopy (FTIR), UV–Visible spectroscopy, X-ray diffraction (XRD), scanning electron microscopy and energy dispersive spectroscopy (SEM–EDS), X-ray photoelectron spectroscopy (XPS) and transmission electron microscopy (TEM) techniques. Furthermore, the antimicrobial efficiency of AgNPs was Gram-negative *Escherichia coli* and on Gram-positive *Bacillus cereus* bacteria was studied using the diameter of the inhibition zone in the disk diffusion test.

2 Materials and Methods

2.1 Materials

Halloysite nano clay, curcumin (cur) and ethanol were purchased from Aldrich chemicals co. in USA and silver nitrate was purchased from Merck Specialities Pvt. Ltd. in India. Mill-Q water used in this work was obtained from UNISA in South Africa.

2.1.1 Synthesis of HNTs/cur/AgNPs

For the synthesis of HNTs/cur/AgNPs hybrid material, 1.0 g HNTs was dispersed in 100 mL of 10 mM of $AgNO_3$ solution using sonication for 30 min. The solution was kept in vacuum for five cycles. It is expected that most of the silver ions were anchored in the lumen structure as well as silicate cages of HNTs during vacuum cycles. The silver ion loaded in to HNTs were collected by whatman filtration and then immersed in 100 mg curcumin in

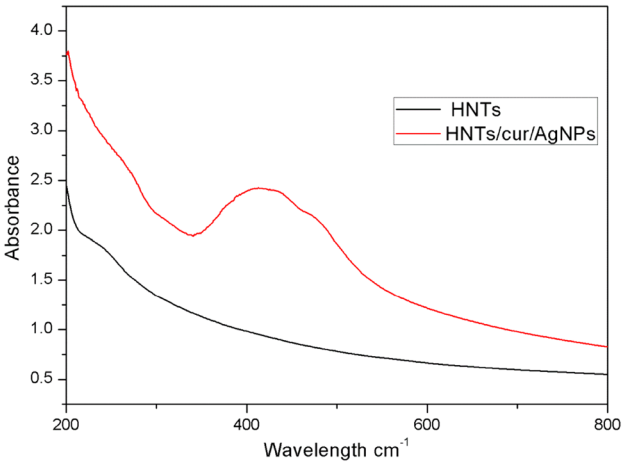

Fig. 2 UV–visible spectrum of HNTs (**a**) and of HNTs/cur/AgNPs (**b**)

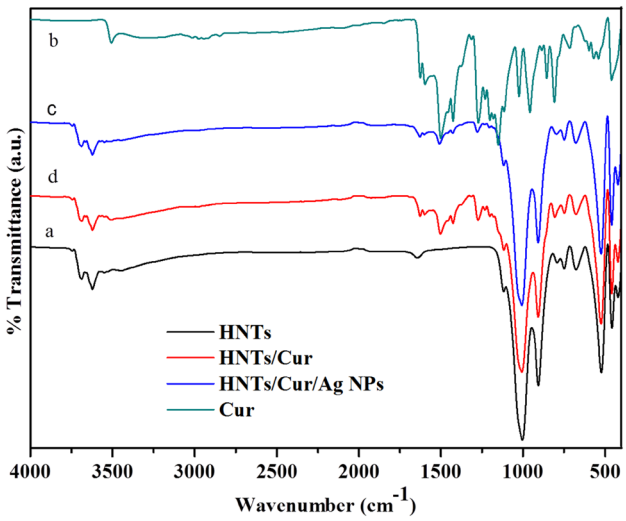

Fig. 1 FTIR spectrum of HNTs (**a**) of curcumin (**b**) of HNTs/cur (**c**) and of HNTs/cur/AgNPs (**d**)

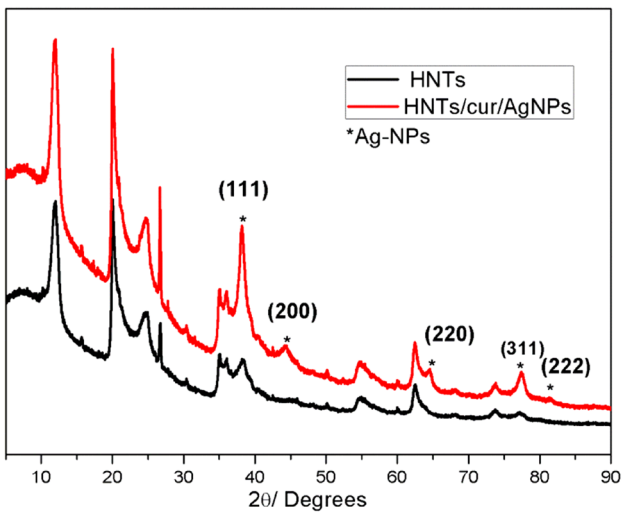

Fig. 3 XRD patterns of HNTs/Cur/AgNPs (**a**) and of HNTs (**b**)

50 mL ethanol solution for 12 h. After 15 min the solution changed color from light yellowish to dark yellowish indicating the formation of AgNPs. The obtained HNTs/cur/AgNPs hybrid material was collected by filtration and dried at 40 °C for 12 h. The same amount of curcumin was added in to the HNTs and designated as HNTs/cur in order to investigate antibacterial performance of curcumin. The characterization details of hybrid nano composite are given in the next section to follow.

2.2 Characterization

The interactions and structural functional groups of HNTs/cur/AgNPs were investigated by a FTIR technique using Wisconsin-410 supplied by Perkin Elmer. UV–Visible spectrophotometer technique was carried out on the synthesised (HNTs and HNTs/cur/AgNPs) using U-2010 machine supplied by HITACHI. XRD technique was used to investigate the crystalline nature of AgNPs in HNTs using AXS D8 supplied by Bruker, recorded over the angular $2\theta = 1.2°–90°$ with scanning rate of 5°/min and CuKa radiation source ($\lambda = 1.54$ Å). The composition and quantification of HNTs/cur/AgNPs were investigated by XPS technique using AXIS Supra™ supplied by Shimadzu, with Al Kα (1486.6 eV) energy source. The morphology and elemental composition of the HNTs/cur/AgNPs were investigated by SEM technique using IT300 supplied by JEOL and EDS technique using X-Max^N supplied by Oxford Ltd, respectively. The morphology and size of AgNPs in the HNTs were investigated by TEM technique using JEM-2010 supplied by JEOL.

2.3 Antibacterial Studies

Anti-bacterial activity of HNTs, HNTs/Cur and HNTs/cur/AgNPs on Gram-negative *E. coli* and gram-positive *B. cereus* bacteria were investigated using disc diffusion method. 100 µL of bacterial culture were uniformly spread on the solidified nutrient agar medium surface of the petri dishes. The samples HNTs, HNTs/cur, HNTs/cur/AgNPs (10 mg/10 mL) were then loaded with sterilized paper discs and placed on the bacterial culture plates. The plates were incubated at 37 °C for 12 h. The inhibition zone was measured around the disc as the antibacterial effect of hybrid materials.

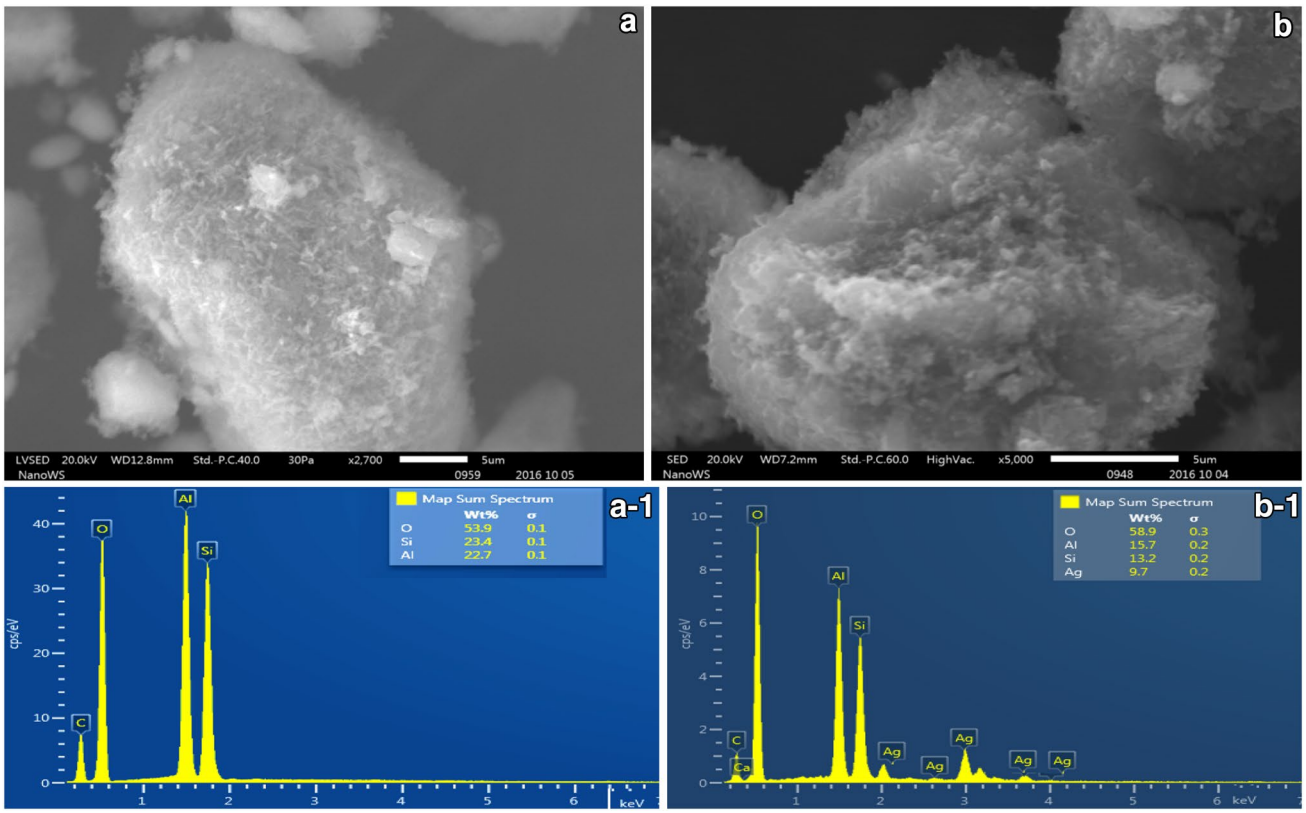

Fig. 4 SEM images of HNTs (**a**), of HNTs/cur/AgNPs (**b**) and their EDS spectra of HNTs (**a-1**) and of HNTs/cur/AgNPs (**b-1**)

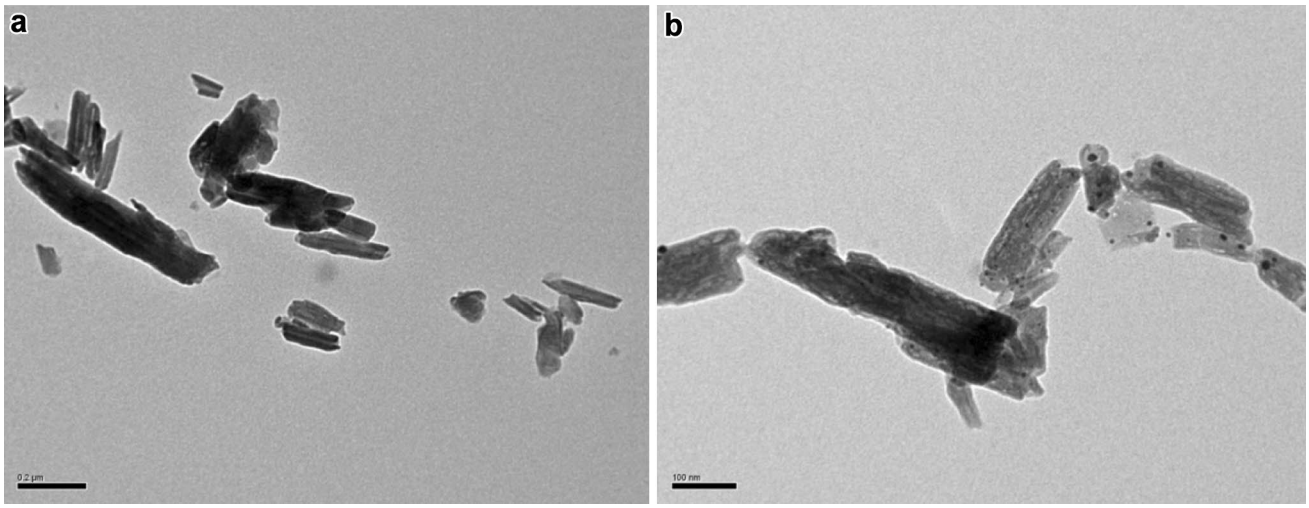

Fig. 5 TEM images of HNTs (**a**) and of HNTs/cur/AgNPs (**b**)

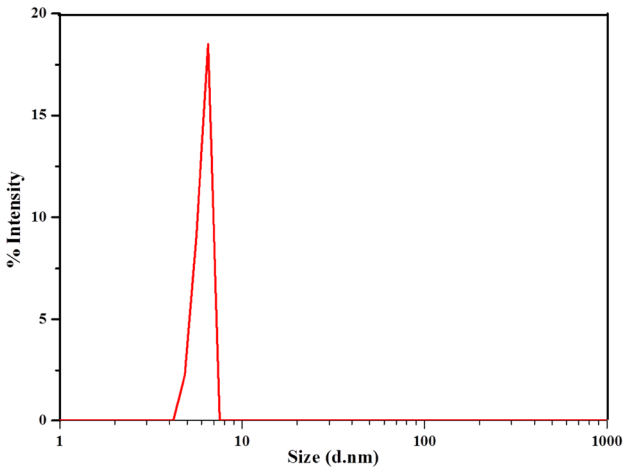

Fig. 6 DLS images of AgNPs

3 Results and Discussions

Highly biocompatible halloysite material was used as a supporting for stability of AgNPs [22]. Curcumin was used as a reducing agent and also possess bacterial activity on gram positive and gram negative bacteria. Subsequently, in the present study, silver ions (Ag^{+}) are reduced by the curcumin to form silver (Ag^{0}) nano particles in the HNTs. The AgNPs are formed in the lumen empty space and also in the silicate cage of HNTs. The obtained nano clay material is cost effective for enhancing the bacterial activity on Gram-positive and on Gram-negative bacteria. The intercalation, formation, crystallinity and morphology of AgNPs in the HNTs were studied and their antibacterial performance was presented in this work.

3.1 FTIR

Figure1 shows the FTIR spectra of pure HNTs (a) of curcumin (b) of HNTs/cur (c) and of HNTs/cur/AgNPs (d). The spectrum of pure HNTs in Fig. 1a shows two intensive bands at 3619 and 3446 cm^{-1} corresponding to the O–H stretching of inner hydroxyl groups and inner surface hydroxyl groups, respectively. The bands at 1120 and 1007 cm^{-1}, respectively confirm apical Si–O and Si–O–Si stretching vibrations. The bands at 732 and 678 cm^{-1} were derive from the perpendicular Si–O stretching vibration. The O–H deformation vibration of inner Al–O–H groups generates the band at 912 cm^{-1}. The spectrum of curcumin in Fig. 1b shows the peaks at 3509 and at the region range from 1450 to 1630 cm^{-1}. These peaks correspond to –OH, C=O and C=C (enol) groups respectively. The peaks observed at 2845, 3015 and in the ranging between 1000 and 1300 cm^{-1}. These peaks correspond to –CH (methyl) –CH (aryl) and C–O–C group respectively. All the peaks are attributed to symmetric and asymmetric configuration of C–O–C chain [35]. In Fig. 1c the spectrum of HNTs/cur shows intensive peaks at 1508, 1427 and 1272 cm^{-1}. These peaks correspond to CO– stretching of enol and phenol groups. The spectrum of HNTs/cur/AgNPs in Fig. 1d also shows the presence of enol and phenol groups in HNTs/cur/AgNPs. The spectrum of the intensive peaks has however, decreased due to the presence of silver particles in the HNTs. These results indicate that HNTs interact with the curcumin in the presence of AgNPs.

3.2 UV-Spectroscopy

The formation of silver nanoparticles in HNTs was determined by UV–Visible spectroscopy technique. Figure 2a

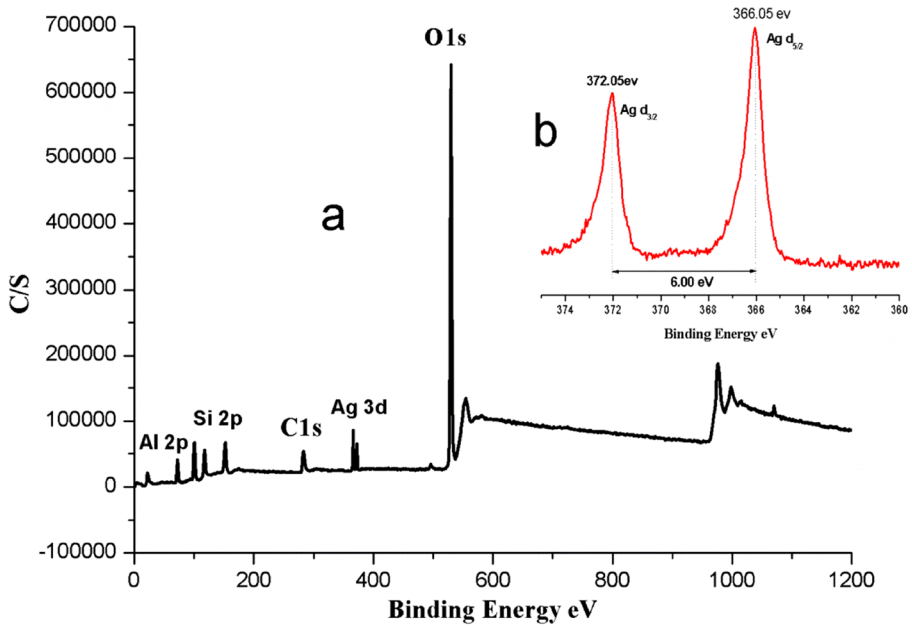

Fig. 7 XPS spectrum of HNTs/cur/AgNPs of Binding energy (**a**) and region of Ag 3d (**b**)

Table 1 XPS analysis of surface composition (%) of elements for HNTs/cur/AgNPs

Elements	XPS (HNTs/cur/AgNPs)	
	Mass concentration (%)	Surface concentration (%)
O 1s	57.66 ± 0.39	70.80 ± 0.33
Si 2p	21.45 ± 0.36	14.94 ± 0.26
Al 2p	19.34 ± 0.39	14.02 ± 0.30
Ag 3d	1.31 ± 0.15	0.24 ± 0.03

shows that there is no plasma peaks associated to pristine HNTs. Figure 2b shows that HNTs/cur/AgNPs has intensive absorption plasma peak at 420 nm indicating a successful formation of AgNPs in the HNTs.

3.3 XRD

Figure 3 shows the XRD patterns of HNTs/Cur/AgNPs (a) and of HNTs (b). The diffractions peaks are observed in the spectrum 2θ values from 20 to 90. The spectrum of HNTs/cur/AgNPs in Fig. 3a shows the intense peaks at 38.16°,

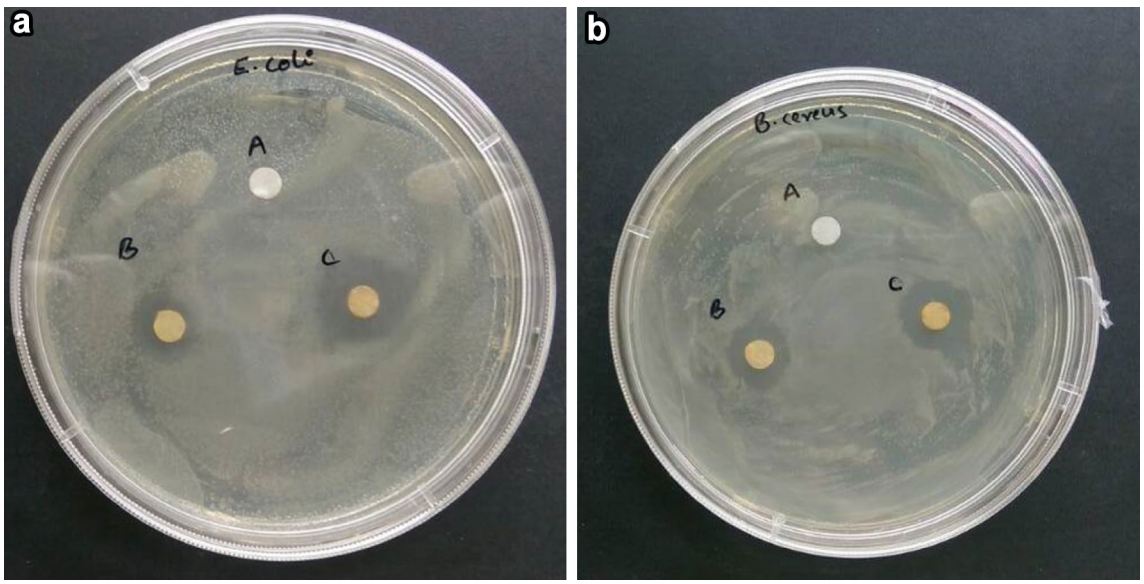

Fig. 8 Antibacterial activity of HNTs, HNTs/cur, and HNTs/cur/AgNPs on both *E. coli* (**a**) and *B. cereus* (**b**)

44.36°, 64.64°, 77.42° and 81.65° with index planes of face cantered cubic of silver at (111), (200), (220), (311) and (222) respectively. These results show the crystalline nature of silver nanoparticles in HNTs. The absence of peaks in Fig. 3b indicates that there is no silver in HNTs.

3.4 SEM–EDS

SEM–EDS technique was used to confirm the formation of AgNPs in HNTs clay. Figure 4 shows SEM images of HNTs (a) of HNTs/cur/Ag-NPs (b) and their EDS spectra in figures (a-1) and (b-1). Figure 4a shows that HNTs have hallow tubular structure with even surface area while Fig. 4b indicates a rigid rough surface structure after a sticking of AgNPs. The HNTs/cur/AgNPs are aggregated, since silver particles are captured in the HNTs by the interaction hydrogen bonding and curcumin phenolic molecules. The spectrum of HNTs 4(a-1) indicates only O, Si, and Al while that of HNTs/cur/AgNPs 4(b-1) indicates O, Si, Al and Ag compositional elements in HNTs after loaded with silver particles.

3.5 TEM

The formation and distribution of AgNPs via insitu reduction method in the lumen structure as well as surface cage of HNTs were confirmed by TEM image analysis. As shown in Fig. 5a the TEM images of pristine HNTs show empty lumen structure. TEM images of HNT/cur/AgNPs in Fig. 5b show that the formation of highly distributed AgNPs in the lumen structure as well as surface cage of HNTs with spherical shape. The spherical shape of AgNPs is due to curcumin having phenolic hydroxyl groups involved during the formation of stable spherical AgNPs. DLS analysis in Fig. 6 shows the size of the extracted AgNPs to be ~5 nm. This is within acceptable range.

3.6 XPS

XPS pattern has been analyzed to confirm the presence of AgNPs in HNTs. Figure 7 shows XPS spectrum of HNTs/cur/AgNPs of Binding energy (a) and high resolution region of Ag 3d (b). Figure 7a indicates that HNTs/cur/AgNPs hybrid material with compositional elements of O-1s, Si-2p, Al-2p and Ag-3d. Figure 7b shows high resolution of Ag 3d region. It was demonstrated that the 3d region has been splitted into two regions such that Ag 3d5/2 and Ag 3d3/2 are located at 367.0 and 373.0 eV using the splitting energy of 6.0 eV. The results confirm the stability of AgNPs in HNTs. The surface and mass concentration of compositional elements is shown in Table 1. The concentration of Ag atom has been evaluated to be 0.24% on the surface of halloysite. Mass concentration % of Ag atom was found to be ±1.31 in HNTs. It can be concluded that AgNPs in the halloysite clay has been formed by using curcumin as reducing agent via insitu reduction.

3.7 Antibacterial Activity

Figure 8 shows antibacterial activities of HNTs (A), HNTs/cur (B) and HNTs/cur/AgNPs (C) on both of *E. coli* and *B. cereus*. It can be seen in both case that the pristine HNTs has no inhibition ability. The ability of HNTs/cur can be noticed with radial inhibition zone of 8 mm for *E. coli* and 13 mm for *B. cereus*. The radial inhibition zone of HNTs/cur/AgNPs is higher than that of HNTs/cur for both *E. coli* (17 mm) and *B. cereus* (16 mm). In general the results show that HNTs/cur the antibacterial activity lower than that of HNTs/cur/AgNPs. Thus, the antibacterial activity was found to be more improved after an introduction of AgNPs in the compound. The resulted HNTs/cur/AgNPs hybrid material has a potential antibacterial activity on both *E. coli* and *B. cereus* and it is suitable for biomedical applications.

4 Conclusion

In this present work, the synthesis of AgNPs in HNTs has a distinct advantage over chemical methods such as simple two steps process, non-toxic, eco-friendly, cost-effective and easy synthesised. A highly uniform spherical shape of AgNPs was introduced via insitu reduction method in the lumen structure as well as surface silicate cage of HNTs. The combination of curcumin and AgNPs in HNTs nanohybrid system was effective to antibacterial activity towards both Gram-positive and Gram-negative bactericide. Hence, the hybrid systems could be administered directly and effectively for antibacterial infections.

Acknowledgements The first author is highly grateful to the University of South Africa for postdoctoral research fellowship.

References

1. Y. Liu, Z. Liu, G. Wang, J. Cryst. Growth **252**, 213 (2003)
2. Y. Wu, P. Yang, J. Am. Chem. Soc. **123**, 3165 (2001)
3. G. Shen, D. Chen, K. Tang, Y. Qian, J. Cryst. Growth **252**, 199 (2003)
4. P. Dallas, V.K. Sharma, R. Zboril, Adv. Colloid Interface Sci **166**, 119 (2011)
5. A.J. Haes, S.L. Zou, G.C. Schatz, R.P. Van Duyne, J. Phys. Chem. B **108**, 6961 (2004)
6. T. Huang, P.D. Nallatham, X.H.N. Xu, J. Am. Chem. Soc. **130**, 17095 (2008)
7. W.K. Jung, H.C. Koo, K.W. Kim, S. Shin, S.H. Kim, Y.H. Park, Appl. Environ. Microbiol. **74**, 2171 (2008)
8. M. Guzman, J. Dille, S. Godet, Nanomedicine **8**, 37 (2012)

9. X. Ding, H. Wang, W. Chen, J. Liua, Y. Zhang, RSC Adv. **4**, 41993 (2014)
10. J. Zhang, Y. Zhang, Y. Chen, L. Du, B. Zhang, H. Zhang, J. Liu, K. Wang, Ind. Eng. Chem. Res. **51**, 3081 (2012)
11. Y. Zhang, Y. Chen, H. Zhang, B. Zhang, J. Liu, J. Inr. Biochem. **118**, 59 (2013)
12. S.T. Zhang, R.W. Fu, D.C. Wu, W. Xu, Q.W. Ye, Z.L. Chen, Carbon **42**, 3209 (2004)
13. S.J. Park, B.J. Kim, J. Colloid Interface Sci. **282**, 124 (2005)
14. X. Lu, T. Imae, J. Phys. Chem. C **111**, 2416 (2007)
15. H.H. Patterson, R.S. Gomez, H.Y. Lu, R.L. Yson, Catal. Today **120**, 168 (2007)
16. W. Gac, A. Derylo-Marczewska, S. Pasieczna-Patkowska, N. Popivnyak, G. Zhkocinski, J. Mol. Catal. A **268**, 15 (2007)
17. A. Murugadoss, A. Chattopadhyay, Nanotechnology **19**, 015603 (2008)
18. J.L. Chen, X.F. Tang, J.L. Liu, E.S. Zhan, J. Li, X.M. Huang, W. Shen, J. Chem. Mater **19**, 4292 (2007)
19. T. Ung, L.M. Liz-Marzan, P. Mulvaney, J. Phys. Chem. B **103**, 6770 (1999)
20. T. Hirakawa, P.V. Kamat, J. Am. Chem. Soc. **127**, 3928 (2005)
21. X.M. Sun, Y.D. Li, Langmuir **21**, 6019 (2005)
22. V. Vergaro, E. Abdullayev, Y.M. Lvov, A. Zeitoun, R. Cingolani, R. Rinaldi, S. Leporatti, Biomacromolecules **11**, 820 (2010)
23. G. Kiani, M. Dostali, A. Rostami, A.R. Khataee, Appl. Clay Sci. **54**, 34 (2011)
24. S. Barrientos-Ramirez, G. Montes de Oca-Ramírez, E.V. Ramos-Fernandez, A. Sepulveda-Escribano, M.M. Pastor-Blas, A. Gonzalez-Montilel, Appl. Catal. A Gen. **406**, 22 (2011)
25. S.M. Lee, K.C. Song, B.S. Lee, Korean J. Chem. Eng. **27**, 688 (2010)
26. P.K. Khanna, N. Singh, S. Charan, A.K. Viswanath, Mater. Chem. Phys. **92**, 214 (2005)
27. V. Thomas, M.M. Yallapu, B. Sreedhar, S.K. Bajpai, J. Colloid Interface Sci. **315**, 389 (2007)
28. H. Noritomi, N. Igari, K. Kagitani, Y. Umezawa, Y. Muratsubaki, S. Kato. Colloid Polym. Sci. **288**, 887 (2010)
29. A. Tripathy, A.M. Raichar, N. Chandrasekaran, T.C. Prathna, A. Mukherjee, J. Nanopart. Res. **12**, 237 (2010)
30. A.K. Jha, K. Prasad, A.R. Kulkarni, Colloid Surf. B **73**, 219 (2009)
31. N. Annamalai, R. Thavasi, S. Vijayalakshmi, T. Balasubramanian. World J. Microbiol. Biotechnol. **27**, 2111 (2011)
32. K. Sudhakar, K. Madhusudana Rao, M.C.S. Subha, K. Chowdoji Rao, E. Rotimi Sadiku, Des. Monomer and Polym. **18**, 705 (2015)
33. A. Kumar, S. Dogra, A. Prakash, Behav. Brain Res. **205**, 384 (2009)
34. S.C. Gupta, S. Patchva, B.B. Aggarwal, AAPS J **15**, 195 (2013)
35. S. Hatamie, M. Nouri, S.K. Karandikar, A. Kulkarni, S.D. Dhole, D.M. Phase, S.N. Kale, Mater. Sci. Eng. C **32**, 92 (2012)